Article

Post-High-Temperature Exposure Repeated Impact Response of Steel-Fiber-Reinforced Concrete

Sallal R. Abid [1,*], Ahmmad A. Abbass [2], Gunasekaran Murali [3,*], Mohammed L. J. Al-Sarray [1], Islam A. Nader [1] and Sajjad H. Ali [1]

1 Department of Civil Engineering, Wasit University, Kut 52003, Iraq
2 Building and Construction Materials Department, Shatrah Technical Institute, Southern Technical University, Shatrah 64007, Iraq
3 Peter the Great St. Petersburg Polytechnic University, 195251 Saint Petersburg, Russia
* Correspondence: sallal@uowasit.edu.iq (S.R.A.); murali_22984@yahoo.com (G.M.)

Abstract: The response of plain and fibrous concrete to the scenario of fired structures exposed to repeated impacts from falling fragmented building elements and other objects is experimentally investigated in this study. The experimental program included the casting and testing of specimens with 0%, 0.5%, and 1.0% hooked-end steel fibers (SFs) under the ACI 544-2R repeated-impact test. The impact test was conducted using cylindrical disk specimens, while 100 mm cubes were used to evaluate the residual compressive strength and weight loss. From each mixture, six disks and three cubes were heated to high temperatures of 200, 400, and 600 °C, while a similar set of specimens were tested without heating as a reference group. The results show that SF could significantly improve cracking impact resistance and dramatically boost failure impact numbers. The retained percentage improvements were the highest for specimens heated to 600 °C, which were approximately 250% at the cracking stage and 1680% at the failure stage for specimens with 1.0% SF. The test results also show that the repeated-impact resistance dramatically deteriorated at high temperatures, where the maximal residual cracking and failure impact numbers after exposure to 200, 400, and 600 °C were approximately 20% and 40%, 4% and 7%, and 2.2% and 4%, respectively.

Keywords: repeated impact; drop weight; high temperatures; fire; steel fiber

1. Introduction

The number of yearly fires that are classified as accidental structural fires is globally shocking. Between 1993 and 2016, there were millions of recorded fires every year, where in approximately 30 to 50 countries, the recorded yearly fires in this period were in the range of 2.5 to 4.5 million with an average of 3.7 million. Within the specified period, approximately 90 million fires were reported, and more than a million death incidences were recorded [1]. For instance, in 2016, the recorded fires in the United States were more than 1,300,000 incidents, while more than 200,000 fires were recorded in the same year in countries such as the United Kingdom, Italy, and France [1]. The high percentage of these fires reaching 40% could classify them as structural fires [2]. Concrete structures have better safe endurance when exposed to fire temperatures compared to metallic and wooden structures. However, catastrophic failure due to the degradation of concrete is possible in many cases. The deterioration of concrete microstructures is directly related to the thermal properties of the adopted mixture materials and the level of high-temperature exposure, where mixtures with different aggregate types behave differently under such conditions [3–8]. In most cases, the exposure to temperatures lower than 200 °C either has a minor effect on the compressive strength of concrete or positively influences it [9–12], while exposure to temperatures higher than 500 °C seriously impacts the compressive strength of concrete [13–17]. On the other hand, it was frequently reported in the literature that the tensile, flexural, and shear strengths of concrete deteriorate at a faster rate than compressive

strength does [18–24]. The main alteration of the microstructural response of concrete starts after reaching a temperature of 350 to 400 °C. At such temperatures, the aggregate exhibits a noticeable expansion that is associated with the opposite contraction of the surrounding cement paste. The reversed thermal movements of aggregate and cement paste accelerate the deterioration of the bond connecting them, which is a source of unfavorable strength deterioration [8,9,13]. Another source of strength deterioration at this range of temperature is the degradation of the aggregate itself and the decomposition of the hydrated products of the cement matrix [13–16]. These thermal actions initiate the quick drop in the strength of concrete and the structural response of the subjected members.

The impact strength of concrete is a design concern in some structures such as the downstream parts of stilling basins where the hydraulic jump needs to be retarded, plane landing runways in airports where tire impact is an important effective load, and military facilities in conflict areas [25–28]. Other typical residential, service, and commercial structures are not usually designed for such loading types. However, some are expected to be subjected to impact loads during the construction period or their lifespan. The accidental falling of construction materials and objects from higher stories is an expected impact load on slabs or beams during construction. On the other hand, cars in parking garages may repeatedly impact the vertical columns and walls [29–31]. Two typical experimental tests are used to evaluate impact loads due to falling objects or the collision of objects with concrete members. The first is the most widely used drop-weight impact test, in which a slab or beam specimen is held horizontally, and a free-falling mass is dropped causing an impact force on its top surface. In this test, full instrumentation is required to measure the impact forces, displacement (deflection), strain, and vibration [32–37]. The second widely used test is the Charpy pendulum impact test [38–40]. ACI 544-2R [41] introduced a simpler and cheaper impact test to evaluate the performance of concrete under low-velocity drop-mass impact. The test is not intended to give quantitative measurement of the impact strength, but it can qualitatively compare the impact performance of different types of concrete mixtures or the effect of different additives on the impact response of concrete. The advantage of the test is that it is applied on small concrete disk specimens and does not require any sophisticated sensors or electronic sampling and measurement tools. Thus, it introduces a low-cost choice to evaluate and compare the performance of different concrete mixtures under repeated fall-mass impacts. This test was extensively used in the last few years to evaluate the impact resistance of different types of fibrous concrete mixtures [42–48].

Several research works were conducted on disk specimens using the ACI 544-2R repeated-impact test to evaluate the impact resistance of plain and fibrous concrete. Different fiber types were considered in mono and hybrid combinations in different recent and traditional concrete composites. Synthetic fibers such as polypropylene fibers [49–52] and polyvinyl alcohol fibers [53,54] were investigated by many previous studies, while steel fibers (SFs) were among the most investigated types of fiber reinforcement because of their ability to boost the resistance of concrete to impact loads. There is wide agreement in the literature that SFs are significantly superior in enhancing the impact performance of concrete mixtures compared to polypropylene and other fiber types. The size and configuration of the investigated SFs were also different in the available literature. In some previous studies, crimped SFs were used [55–58]; in other studies, hooked-end SFs were adopted [59–70]; in others, hooked-end crimped SFs were tested [71–76]. On the other hand, straight coated SFs were utilized in self-compacting [77,78] and high-performance [79,80] concrete mixtures. The repeated impact performance of concrete mixtures incorporating other types of SFs such as sheared steel sheets and straight wires was also reported by an earlier study [81]. All previous studies agreed that using SFs with small volume dosages of less than 1.0% noticeably improves the impact performance of the tested samples, while using 1.0% and higher SFs could boost resistance to cracking and failure by several times under repeated impacts compared to plain specimens.

In spite of the considerable research literature on the repeated impact of fiber-reinforced concrete, very few works are available on their post-fire-exposure behavior. Mehdipour et al. [82] investigated the repeated-impact strength of rubberized concrete that includes metakaolin after exposure to high temperatures. The authors incorporated crumb rubber in an approximately similar quantity in all mixtures in addition to 0.25 to 1.0% of SFs. Three sets of mixtures were adopted depending on the percentage replacements of cement by metakaolin of 0%, 10%, and 20%. The specimens were subjected to temperature levels of 150, 300, 450, and 600 °C. The authors reported a significant drop in cracking and failure impact numbers after exposure to temperatures of 150 and 300 °C, which exceeded 50% in most cases. Further degradation was recorded after exposure to 450 °C, while the impact strength almost vanished at 600 °C. Al-Ameri et al. [83] conducted an experimental study to investigate the influence of exposure to temperatures of 100, 200, 300, 400, 500, and 600 °C on the ACI 544-2R repeated impact of conventional plain concrete. They reported that exposure to 100 °C had a negligible effect on impact strength, while a strength drop of approximately 75% was recorded for specimens subjected to 200 °C. Exposure to temperatures of 300 and 400 °C led to additional strength deterioration, while the strength almost faded at temperatures of 500 °C and higher. In other studies, Al-Ameri et al. studied the residual repeated-impact performance of engineered cementitious composites (ECC) after exposure to subhigh temperatures [84] and high temperatures up to 600 °C [85]. The mixtures were reinforced with 2% polypropylene fibers. The results of the tests showed that ECC specimens could stand up to 200 °C without exhibiting a significant reduction in impact strength, which was attributed to the presence of polypropylene fibers that had still not melted. On the other hand, the melding of the fibers after exposure to 300 and 400 °C decreased the cracking and failure impact numbers of ECC samples by more than 50%. The retained numbers of impact blows decreased sharply, and the impact resistance faded after heating to 600 °C.

2. Research Significance

As reported in Section 1, despite great efforts to control their causes and effects, accidental fires threaten civil structures and human lives every day, and being exposed to impact loads is possible for different structural members in various structures. The worst is the scenario of a fired structural member that is subjected to multiple impacts from falling fractured parts or objects under catastrophic material deterioration due to fire-elevated temperatures. Failed parts falling from the slab or mechanical equipment falling in the false sail is expected under accidental fires. If fires last for longer before being extinguished, further failures are probable. Thus, the scenario of repeated impacts from fallen parts and objects is expected on already fire-deteriorated concrete structural parts at lower levels. Despite the need to understand the behavior of concrete members under the dual accidental loading of fire and low-velocity repeated impact, very few studies attempted to investigate this issue, and the focus of most of the research was on explosive [86–89] and projectile [90–94] impacts. To better understand the response of concrete structures to such a loading scenario, an experiment was conducted in this study, where conventional concrete with moderate strength was adopted, which is the most widely adopted type of concrete in traditional residential and civil structures, aiming to fill some gaps of knowledge in this area. The incorporation of steel fibers was found in the literature to boost the impact strength of concrete. Its incorporation effect on residual repeated impact was investigated in a previous study [82], where the adopted mixtures incorporated additional materials such as crumb rubber. Thus, the residual response was affected by several influencing parameters and not only steel fibers. Therefore, the experiment of this study was designed to evaluate the sole effect of steel fibers on the response of conventional concrete to dual fire and repeated-impact loading.

3. ACI 544-2R Repeated-Impact Test

ACI 544-2R [41] introduces a simple impact test that does not include any sort of sophisticated sensors or data acquisition systems. Simply, it is only required to record the number of repeated impacts that cause a visible surface crack on the specimen, and then the number of impacts required to split a specimen till failure. These numbers are recorded and used to compare the different tested mixtures. The test apparatus for the repeated-impact test is depicted in the sketch shown in Figure 1. The apparatus was composed of a 4.54 kg drop steel mass that was dropped from a height of 457 mm onto a steel ball placed on the top surface of the concrete test specimen. The specimen was a cylindrical disk with a diameter of approximately 150 mm and a thickness of approximately 63 mm. The steel ball had a diameter of approximately 63 mm and was held in place using a steel ring that was attached to a special holding system, as shown in Figure 1. The specimen was prevented from rebounding during the impact testing using four steel holding plates (lugs). Elastomer pieces were inserted between the steel lugs and test specimens to prevent any possible movement of the specimens. The load was then released to repeatedly drop on the steel ball. The number of impact blows required to initiate the surface cracking of the test disk was recorded as the cracking number of impact (Ncr). The elastomers were then removed, and impacting continued. When the crack was widened so that at least three of the four holding lugs were touched by the specimen, the specimen was considered to have failed, and the number of impact blows was recorded as the failure impact number (Nf).
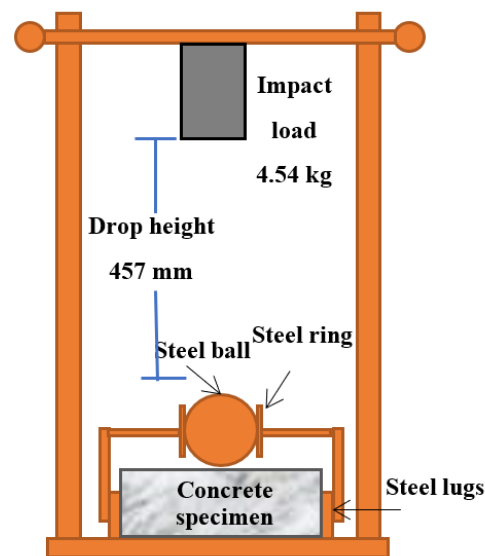

Figure 1. Testing apparatus of the ACI 544-2R repeated-impact test.

4. Experimental Program

The main focus of the work presented in this article is the experimental impact testing of steel fiber-reinforced concrete after high-temperature exposure. Therefore, a concrete mixture with moderate strength and three levels of fiber reinforcements was prepared. Ordinary Portland cement type 42.5 was used in the mixtures, and it had the chemical and physical properties listed in Table 1. Crushed gravel from Wasit province in the central Iraq region was used as a coarse aggregate. Similarly, natural sand from the same region was adopted as a fine aggregate. The maximal particle size of the gravel was 12.5, while the fineness moduli of the gravel and sand were 5.75 and 2.46, respectively. The sieve analysis of both aggregate types is shown in Figure 2. Hooked-end steel fiber with 0.5 mm diameter and 35 mm length was used. The tensile strength of the used steel fiber was 1200 MPa, while its appearance is shown in Figure 3. Fibers noticeably influence the workability of concrete mixtures. Therefore, to enhance the workability, liquid-state superplasticizer Sika® ViscoCrete SP 5930-L (Dubai, UAE) was used. Three concrete mixtures, M0, M0.5, and M1.0,

were prepared with the same cement and water quantities, but with different volumetric fiber dosages of 0%, 0.5% and 1.0%, respectively. Table 2 shows the details of the concrete mixtures of this study.

Table 1. Properties of the used Portland cement.

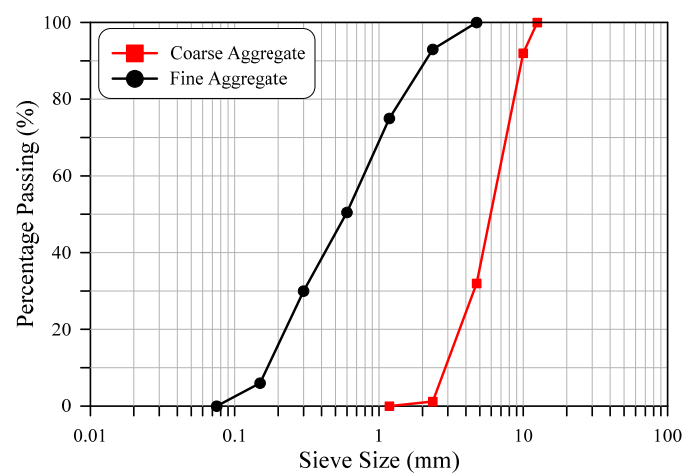| Chemical Composition (%)					
SiO_2	Fe_2O_3	Al_2O_3	CaO	MgO	SO_3
20.1	3.6	4.58	61.4	2.12	2.65
Physical Properties					
Loss on Ignition (%)		Specific Surface (m^2/kg)		Specific Gravity	
1.37		368		3.15	

Figure 2. Particle grading of aggregates.

Figure 3. Used hooked-end steel fibers.

Table 2. Concrete mixtures (kg/m^3).

Material	M0	M0.5	M1.0
Cement	450	450	450
Sand	675	670	665
Gravel	990	982	974
Water	207	207	207
Steel fiber	0	39.25	78.5
Superplasticizer	0.74	1.3	1.7

From each mixture, 24 cylindrical specimens (disks) with 150 mm diameter and 63 mm thickness were prepared and cast together with 12 concrete cubes with 100 mm side length. The disks were used to carry out the repeated-impact tests, while the cubes were used for compressive strength evaluation. Figure 4 shows the used casting molds, and the cast disk and cube specimens. All specimens were cured in water for 28 days at a curing temperature of approximately 23 °C.

(a)   (b)

Figure 4. Impact and compressive strength specimens. (**a**) Specimen molds; (**b**) Cast specimens.

The 24 disks and 12 concrete cubes from each mixture were each divided into 4 groups of specimens. Three high temperature levels were adopted in this study: 200, 400, and 600 °C. Six disk specimens and three cube specimens from each mixture were subjected to each level of high-temperature exposure. The fourth group of specimens (6 disks and 3 cubes) from each mixture were tested at room temperature without being subjected to high temperatures. Thus, in total, 96 disks and 48 cubes were prepared and tested to evaluate the residual impact and compressive strength of the adopted mixtures. After removal from the water curing tank, the specimens were left in the laboratory environment until the next morning, when a primary drying phase was conducted using an electrical oven. The specimens were placed in the oven for 24 h at a temperature of 105 °C to prevent unfavorable explosive failure while being heated to high temperatures. The heating to the desired high temperatures was conducted at an approximate constant rate of 4 °C/min using the electrical high-temperature furnace shown in Figure 5a. The specimens were placed inside a protection box in the furnace to avoid damaging the furnace interior elements in the case of specimen explosive failure, as shown in Figure 5b. The specimens were heated in small groups of six disks or three cubes to allow for uniform temperature distribution over the specimen surfaces. Each of the temperature levels was reached by considering the above-mentioned heating rate. When the desired temperature level had been reached, the furnace temperature was kept constant at that level to thermally saturate the specimens. Then, the cooling phase was initiated by opening the furnace door to allow for a slow cooling to room temperature, as depicted in Figure 5c.

After completing the heating of the specimens to the required temperature levels, the specimens were tested at an age of approximately 32 days; after the 28 curing days, the drying and heating processes took from 3 to 4 days. The unheated specimens were also tested at the same testing age. The concrete cubes were tested under uniaxial concentric compression using a 3000 kN capacity compressive testing machine. On the other hand, the disk specimens were tested under falling mass impact loads following the procedure recommended by ACI 544-2R [41], where a drop mass of 4.54 kg was dropped from a constant height of 457 mm onto the disk specimens. Instead of using the manually operated repeated-impact testing apparatus, the automatic testing machine shown in Figure 6 was used in this study. As shown in the figure, the machine performs automatic impacts from

the desired height and introduces a digital counting of the number of impacts required to reach the cracking and failure of the specimens. The tester can simply observe the cracking and failure of a specimen using a large monitor that is attached to a high-resolution digital camera focused on the test specimen (Figure 6a).
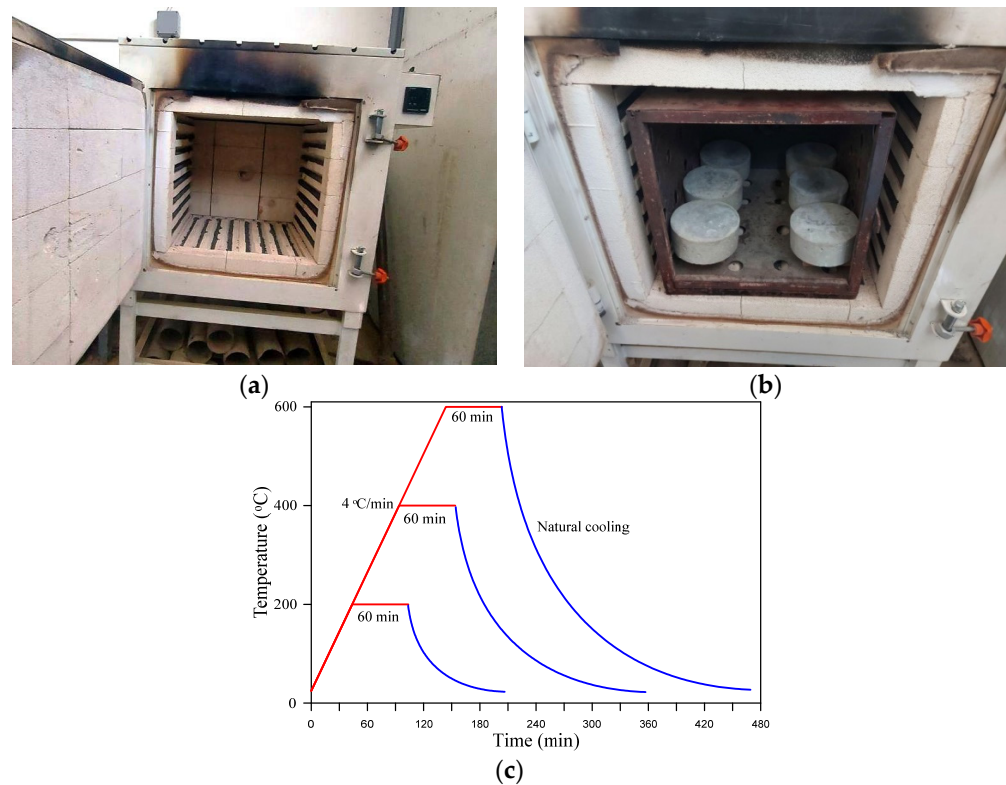

Figure 5. Heating of the test specimens. (**a**) Furnace dimensions; (**b**) Specimen heating; (**c**) Heating scenarios.
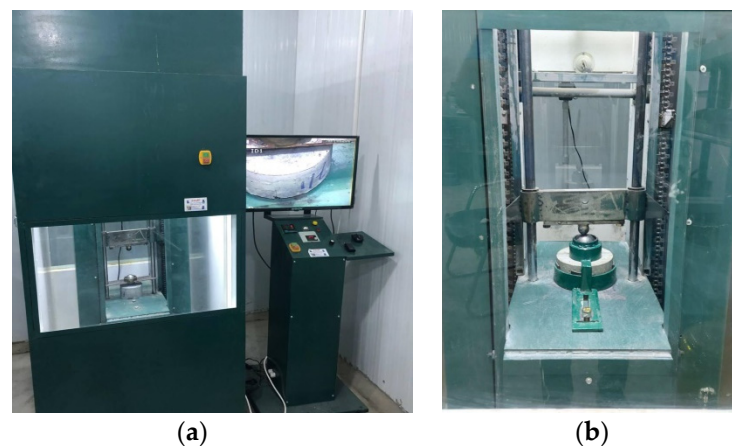

Figure 6. Repeated impact testing. (**a**) Testing machine; (**b**) Specimen testing.

5. Results and Discussion of Control Tests

5.1. Weight Loss

As a control measurement, the weight of the cube specimens was recorded after exposure to each temperature level, and the average of three cube specimens was recorded as the residual weight. The weight loss was then calculated as the difference of this value from the weight of corresponding unheated cubes. The weight loss of the three groups is presented in Figure 7 for the three levels of temperature. The weight of the specimens

was obviously reduced after exposure to all temperature levels regardless of the used fiber content, and this reduction increased with temperature increase. The weight loss at 200 °C was due to the evaporation of the free moisture in the pores between the gel and aggregate particles, while the moisture content absorbed by the gel particles started to decrease at the harsh heating effect of the higher temperatures, leading to further weight loss. After the dehydration of hydrated cement products (after 400 °C), another stage of weight loss was recorded at 600 °C, as revealed in Figure 7. The weight loss of the three fiber contents was in the ranges of 54.8 to 77.8, 92.3 to 119.2, and 115.8 to 156.3 gm after exposure to 200, 400, and 600 °C, respectively.
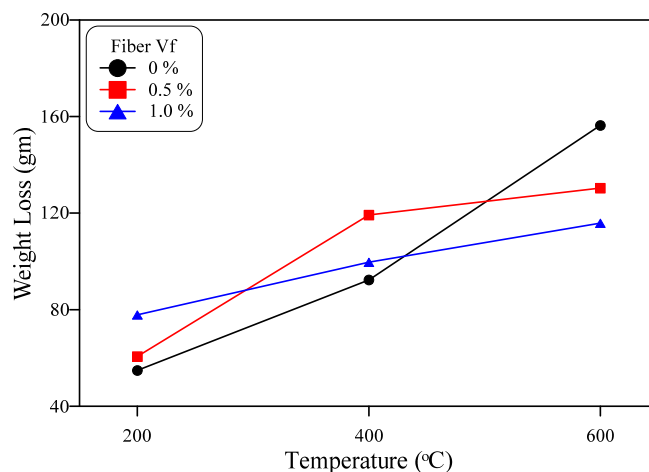

Figure 7. Weight loss of the cube specimens.

5.2. Compressive Strength

The effect of steel fiber on the compressive strength of concrete is a point of disagreement among interested researchers, where previous researchers reported a noticeable to significant development due to SF incorporation, while others reported trivial effects. Figure 8 clearly shows that SF has a positive impact on compressive strength before and after exposure to high temperatures. The increase in compressive strength is clear with the increase in SF content. For the unheated specimens, the compressive strength levels were 40.3, 41.5, and 47.1 MPa for mixtures with 0%, 0.5%, and 1.0% SF, respectively. Hence, the incorporation of 0.5% and 1.0% of SF improved the compressive strength by approximately 3% and 17%, respectively. A similar trend was observed for specimens heated to the adopted high temperatures but with different percentages, where the percentage improvements due to the incorporation of 0.5% and 1.0% SF were approximately 9% and 14% at 200 °C, 23% and 36% at 400 °C, and 32% and 34% at 600 °C, as depicted in Figure 8b–d, respectively. This result means that, in addition to its positive impact at ambient temperature, SF could enhance bridging the material matrix components that were fractured due to exposure to elevated temperatures, which is clear from the higher percentage developments at 400 and 600 °C compared to in the unheated specimens. Steel can sustain a temperature of 600 °C without exhibiting destructive material changes. With their high tensile strength, SFs crossed the fine continuous thermal cracks, which enhanced the internal bond, allowing for sustaining higher compressive loads [20,22].
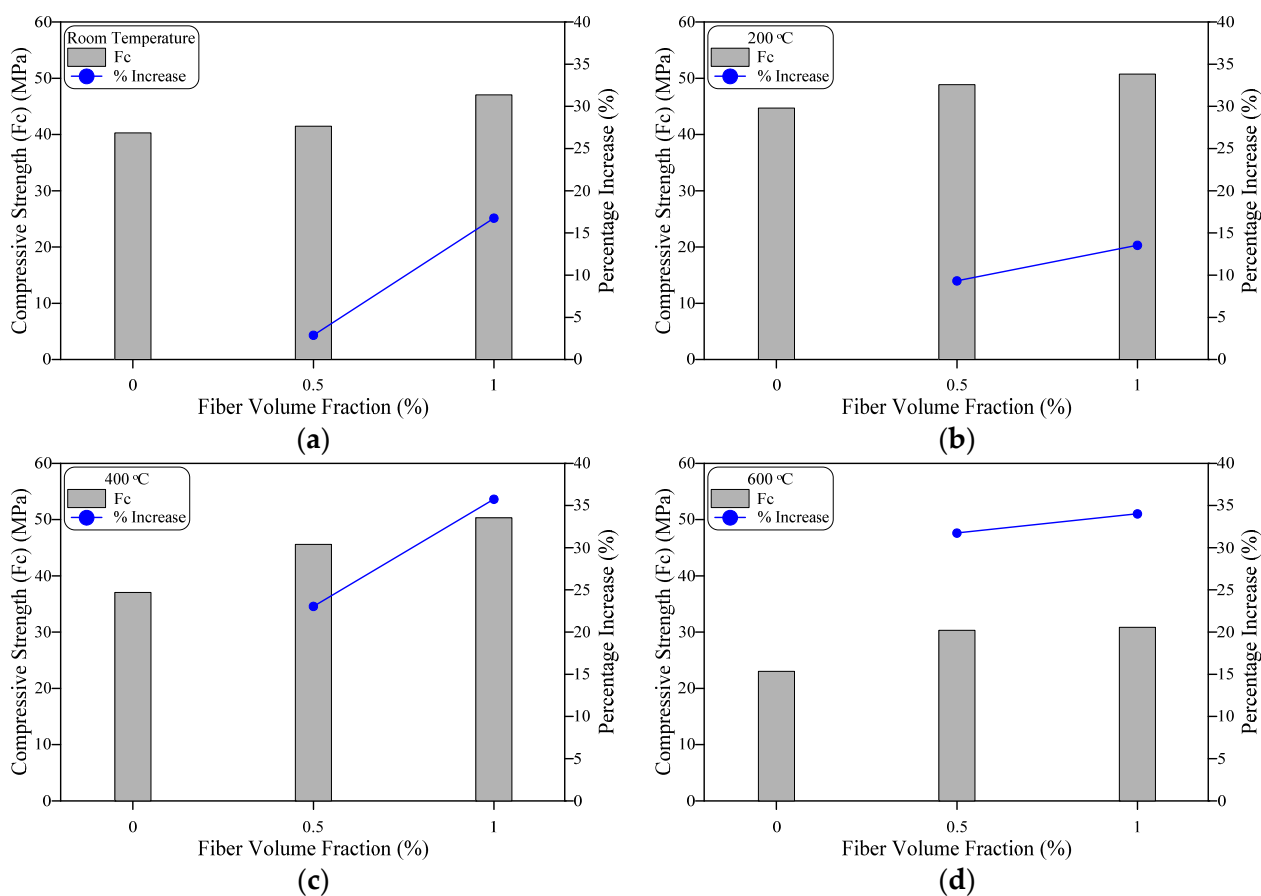
Figure 8. Compressive strength results. (**a**) Room temperature; (**b**) 200 °C; (**c**) 400 °C; (**d**) 600 °C.

The effect of elevated temperatures on compressive strength is better illustrated in Figure 9, which shows the residual strength of the heated specimens. After the specimens had been heated to 200 °C, higher compressive strength was retained regardless of fiber content. The increase in strength between 150 and 350 °C was reported by many previous studies [2,4,13]. The quick evaporation of free moisture from the structure's pores and the cement gel pores increased the attraction of surface forces between the particles of the cement gel, which led to stiffer behavior under compressive stresses [95,96]. As shown in the figure, the three mixtures exhibited a strength percentage increase of 10.9% to 17.8% after exposure to 200 °C compared to the corresponding unheated strength values. The exposure of Portland cement concrete to a temperature of 400 °C initiates the strength steep degradation, where hydrated products suffer a reversed chemical change due to the decomposition of calcium hydroxide [15,20–22]. The differential thermal actions of the cement matrix and aggregate particles, the contraction of the former and expansion of the latter, accelerate the bond deterioration between them, leading to a significant loss of strength [13,97]. These effects at 600 °C are obvious in Figure 9, where the concrete cubes with 0%, 0.5%, and 1.0% SF exhibited percentages of decreases of 42.9%, 26.9%, and 34.5%, respectively. On the other hand, as it is clear in the figure, the presence of SF retarded the strength drop at 400 °C, while a percentage decrease of 8% was recorded for the plain cubes, which is attributed to the SF bridging action as discussed in Figure 8.
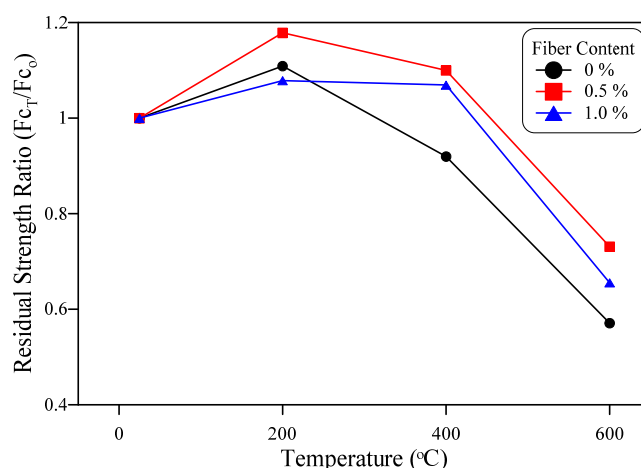
Figure 9. Residual compressive strength after high-temperature exposure.

6. Results and Discussion of Impact Numbers

6.1. Influence of Fiber Content

The results of the repeated impact tests are presented in Figures 10–13 in terms of cracking and failure impact numbers. Figure 10 explicitly shows the role of SF in boosting the impact resistance of the tested disk samples. Figure 10a,b show that SF could duplicate the number of impact blows required to cause the surface cracking of the target specimens before heating and at 200 °C, where the percentage increases in Ncr gained by incorporating 0.5% and 1.0% of SF for the reference (unheated) specimens were approximately 56% and 111%, respectively, compared to the corresponding plain specimens, while Ncr increased by approximately 38% and 142%, respectively, after exposure to 200 °C. On the other hand, corresponding percentage increases of 41% and 47% were recorded for fibrous (0.5% and 1.0%) specimens heated to 400 °C, which is the lowest range of impact strength development recorded in the study. Exposure to 600 °C is expected to cause the most serious damage in the material's microstructure; therefore, Figure 10d shows that the maximal SF efficiency was recorded at this temperature, where the Ncr of specimens with 0.5% and 1.0% SF increased by approximately 117% and 250%, respectively, compared to the corresponding plain disks heated to the same temperature.

SF could obviously improve the cracking impact strength by several times more than compressive strength, although both specimens were subjected to a top surface compression force. The difference is the type of stresses generated in the material due to the applied load. The compression test subjects uniform axial compression stress on the top surface, inducing normal compressive stresses in the material's internal structure. On the other hand, the central compressive impact from the falling mass induces a surface compressive stress that is transformed in the microstructure as a sort of a tensile wave. As concrete is superior in bearing compressive loads and weak in tension, its tensile strength and hence its impact strength were noticeably affected by the presence of SF reinforcing elements that could sustain high tensile stresses. At this stage, the fibers cut the way of many tiny internal microcracks, preventing their extension to the surface. As a result, the impact resistance increased, and the surface cracking was postponed [30,58].
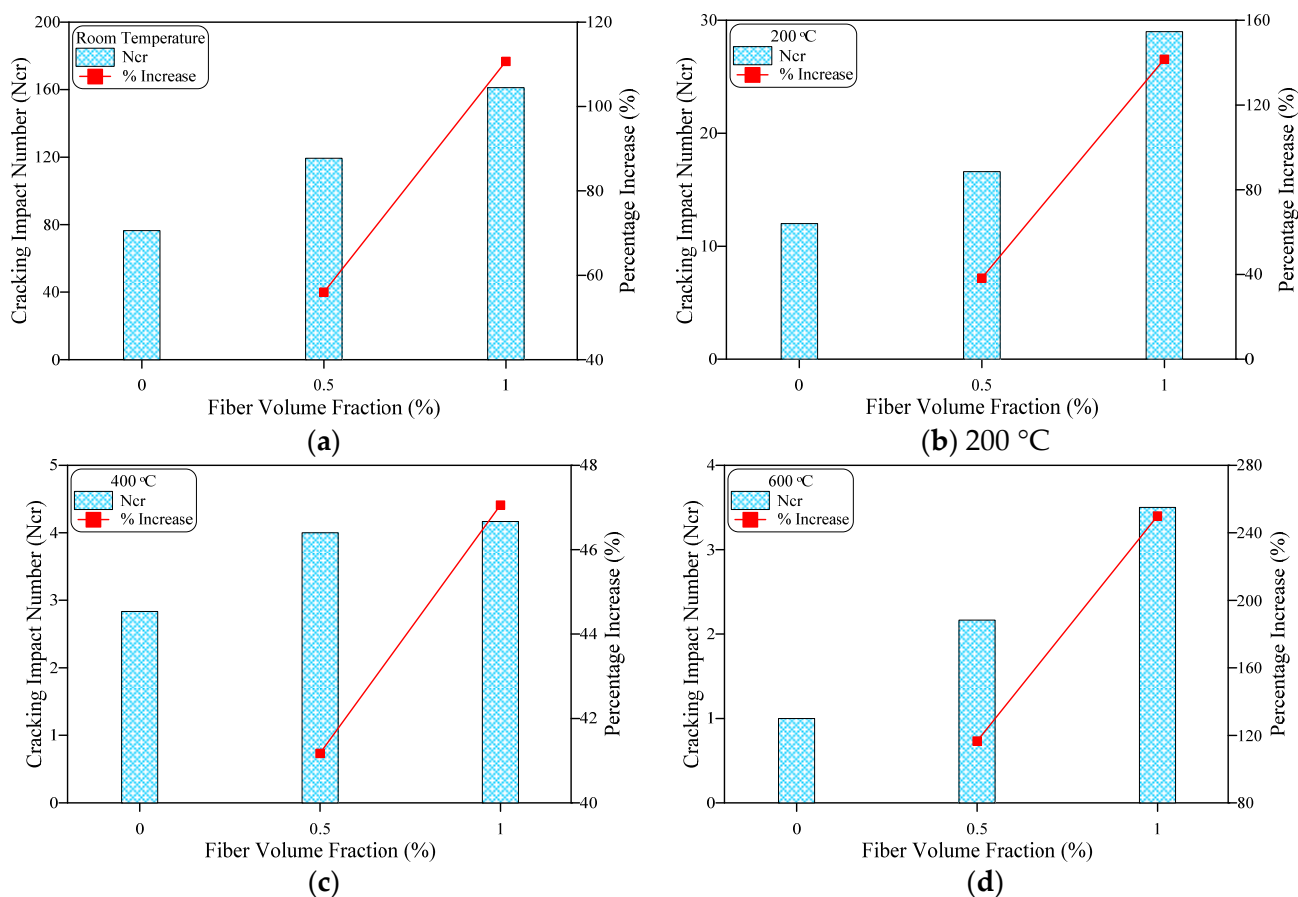
Figure 10. Cracking impact number results of disc specimens. (**a**) Room temperature; (**b**) 200 °C; (**c**) 400 °C; (**d**) 600 °C.

Figure 11 presents the results of the failure impact numbers at ambient temperature and after exposure to high temperatures. The figure shows that using 0.5% of SF caused significant jumps in the failure impact resistance of all specimens (all temperatures) compared to the corresponding plain specimens. The percentage increase in the Nf of the 0.5% fibrous specimens was 151% to 278% for unheated specimens and specimens exposed to 200 and 400 °C. On the other hand, after exposure to 600 °C, the specimens with 0.5% SF could resist 683% higher Nf blows compared to plain specimens heated to the same temperature. The incorporation of 1.0% SF led to much higher-percentage developments in failure resistance against repeated-impact load. The unheated specimens with 1.0% SF could resist approximately 421% higher Nf compared to plain specimens. Similarly, fibrous specimens with 1.0% SF heated to 200, 400, and 600 °C retained higher Nf blows compared to their corresponding plain specimens by approximately 1056%, 648%, and as high as 1683%, respectively (Figure 11b–d). Two conclusions can be drawn from these results. The first is that the effect of fiber at failure is much higher than that at cracking, while the second is that specimens heated to 600 °C exhibited the highest percentage developments at both the cracking and failure stages. Understanding the function of fibers in concrete explains the former note, where fibers work as tiny dispersed reinforcement elements that retard crack propagation and widening. Thus, their real reinforcement role starts after the formation of many cracks inside the matrix, which is the state of postcracking to failure. Hence, before surface cracking, fibers are barely functional, while they are fully functional after cracking, which explains the better performance of SF at the failure stage than that at the cracking stage [73]. On the other hand, the cause of the second conclusion is the degree of cracking that occurred at 600 °C, where the chemical (dehydration of hydrated products) and physical (differential thermal movements) changes deteriorated the microstructure of

the concrete; at such a temperature, SFs were almost fully functional. Therefore, the fibers tried to keep the fractured elements together by crack bridging action, which dramatically raised the retained impact numbers compared to those of the plain specimens.
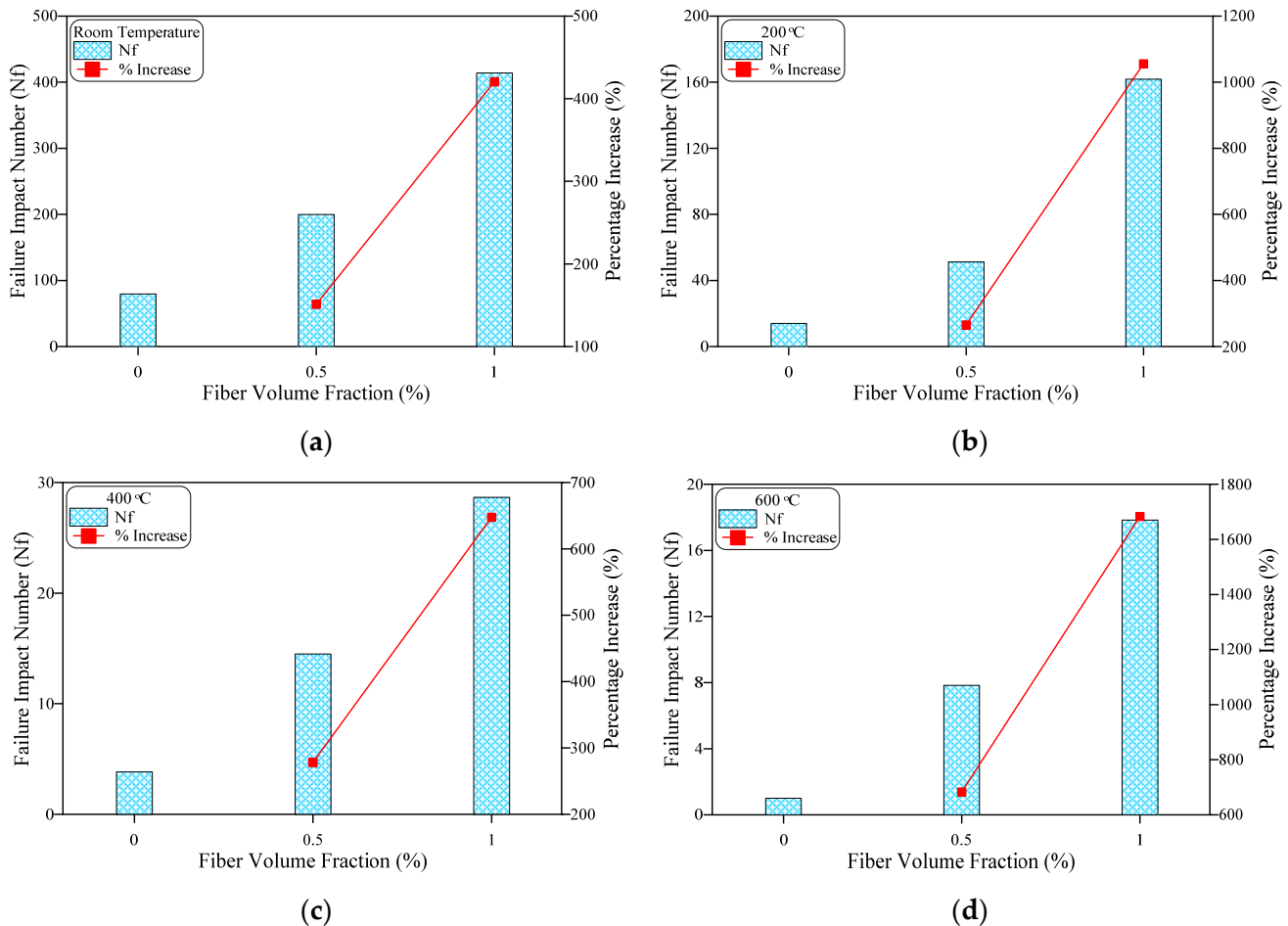

Figure 11. Failure impact number results of disc specimens. (**a**) Room temperature; (**b**) 200 °C; (**c**) 400 °C; (**d**) 600 °C.

6.2. Residual Impact Numbers of Heated Specimens

Figure 12 shows the residual cracking impact number (Ncr_T) after exposure to each temperature level T (200, 400, and 600 °C) for the three mixtures, while Figure 13 shows the residual failure impact records (Nf_T) at each temperature level T. The values of Ncr_T and Nf_T were normalized by their corresponding unheated values Ncr_R and Nf_R. The figures clearly reveal the dramatic drop in impact resistance after exposure to all adopted high temperatures. The cracking and failure impact numbers of the specimens heated to 200 °C exhibited a very sharp decrease, where the residual Ncr was generally lower than 20%, while the residual Nf percentages of the mixtures with 0%, 0.5%, and 1.0% SF were approximately 18%, 26%, and 39%, respectively, compared to their corresponding unheated specimens. Keeping in mind that the compressive strength of cubes heated to 200 °C was higher than that before heating or even barely changed, the steep deterioration in impact resistance explains the different behaviors of heated concrete under the different types of imposed stresses, which highlights the significance of investigating the residual response considering the investigated scenario of fired concrete being subjected to repeated impacts from falling fragments and objects. The behavior of heated concrete under steady compressive stresses due to typical sustained deal loads is not as dangerous as that under accidental impact loads, where shocking tensile waves are induced in the latter within a very short amount of time, which explains the harsh deterioration of the thermally weakened

microstructure and the resulting steep impact strength loss. The impact resistance of specimens heated to temperatures of 400 °C almost vanished for the three mixtures where, as shown in Figure 12, the specimens with 0%, 0.5%, and 1.0% SF could withstand the very few impacts of 2.8, 4, and 4.2, respectively, until they were surface-cracked. Hence, the residual Ncr of the three mixtures (compared to that of the unheated specimens) was generally less than 4%. After cracking, the plain specimen required only one impact blow to fail, recording a residual Nf of approximately 5%, while the fibrous specimens could withstand a few more impact blows before failure due to the bridging action of fibers. However, the residual Nf of these mixtures was only approximately 7% (Figure 13), which reflects a similar degree of harsh deterioration due to exposure to 400 °C. Figures 12 and 13 show that exposure to 600 °C had almost the same effect as that to 400 °C because the impact strength had already almost vanished. Residual Ncr at 600 °C was less than 2.2% for all mixtures, while maximal residual Nf was approximately 4%.

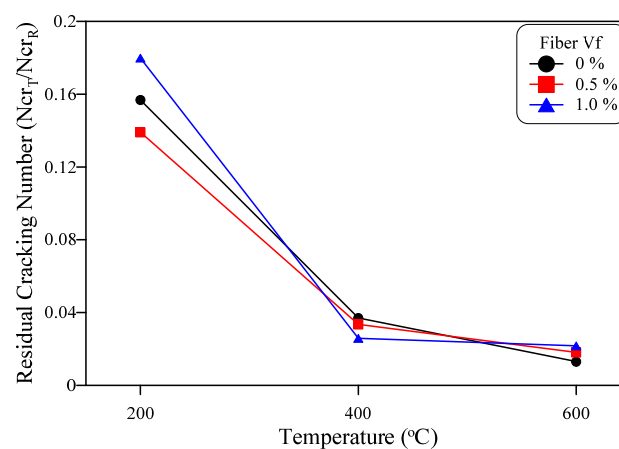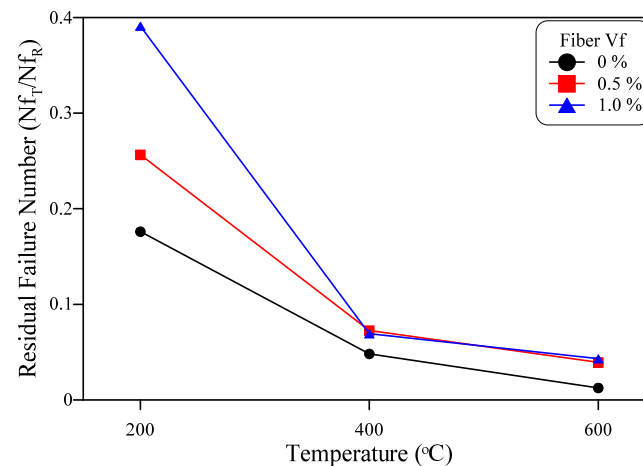**Figure 12.** Residual cracking impact number after high-temperature exposure.

Figure 13. Residual failure impact number after high-temperature exposure.

7. Cracking and Fracturing of Impact Specimens

7.1. Influence of Fiber Content

Figure 14 shows the final failure pictures of the selected specimens from the three mixtures with 0%, 0.5%, and 1.0% FS. The plain specimens (0% FS) exhibited a brittle type of failure. After crack formation, a few additional impact blows (2 to 4) were enough to widen the surface line crack (Figure 14a) or the surface diagonal cracks (Figure 14b). The failure was associated with a small central fracturing zone, as shown in Figure 14b. As concrete is a brittle material, it was not able to withstand the postcracking impact stresses

due to the additional impact blows that had been transferred across the weakest paths (cracks), leading to widening them and causing the brittle failure of the specimens.
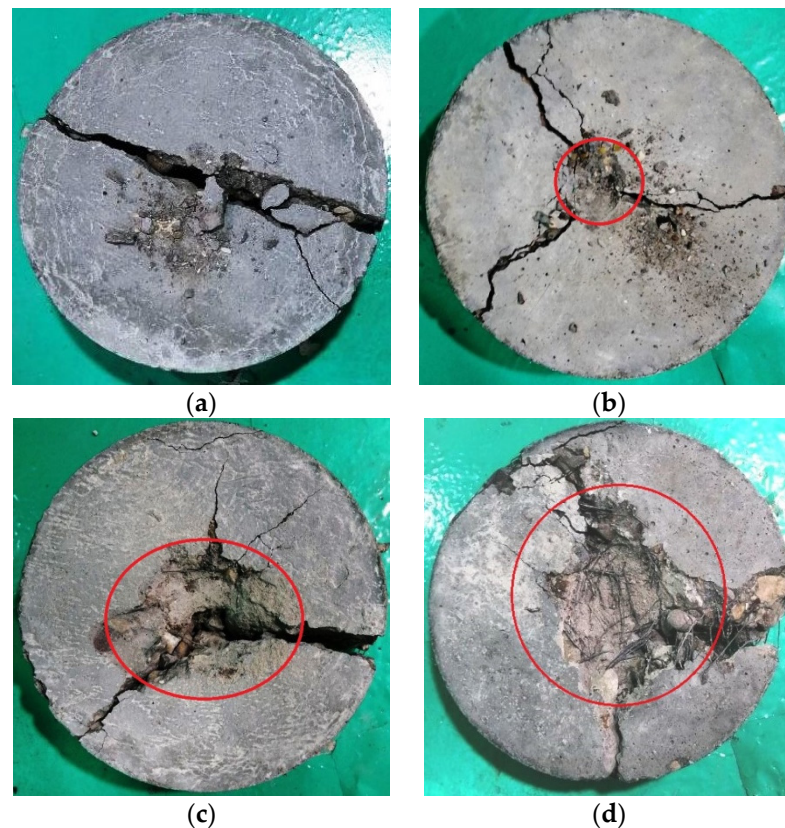

Figure 14. Failure patterns of heated specimens. (**a**) 0% FS line cracking; (**b**) 0% FS diagonal cracking; (**c**) 0.5% FS; (**d**) 1.0% FS.

Fibrous specimens showed continuous behavior under impact loading, where using SF improved the ability of the specimens to absorb higher impact energy, and exhibit ductile cracking and fracturing. As shown in Figure 14c, the central fracturing zone for specimens with 0.5% SF was much larger than that for plain concrete, while it was even wider for specimens with 1.0% FS. The presence of this area was due to the shielding provided by SF to the concrete layers beneath, where fiber groups composed a shadow zone [84] that relieved the forces applied on the inner concrete layers by the central impacting. Hence, the grouped fibers absorbed most of the impact energy, which reduced the stresses on the concrete matrix and aggregate. By applying further impact blows, the SF shielding was weakened, and more stresses were transferred through the subsurface concrete layers, causing a fracture zone that was much wider than that in plain specimens. The bridging of cracks was an additional action of the incorporated SF that enabled the specimens to absorb significantly higher impact energy, and altered the failure to the ductile one shown in Figure 14c,d.

7.2. Influence of High-Temperature Exposure

The failure patterns of the heated specimens are shown in Figure 15. The fracturing patterns of the specimens heated to 200 °C were similar to those of their corresponding unheated specimens shown in Figure 14. The plain specimens exhibited slight central fracturing with diagonal cracks, as shown in Figure 15a, while the fibrous specimens showed significant central fracturing before crack widening (Figure 15d,g). This means that, despite the sharp decrease in impact strength at this temperature, the response of crack formation was not significantly influenced, which reveals that the microstructure was

not very affected by heating to 200 °C (as discussed in Section 6.2), while the deterioration was faster under impact loads. In contrast, the effect of exposure to high temperature was clear on specimens heated to 600 °C where, as shown in Figure 15c,f,i, the thermal cracks on the surface of these specimens were obvious, which noticeably altered the final failure view from the typical ones discussed in Figure 14. The plain specimens at this temperature (Figure 15c) exhibited very fine multidirectional multicracking, revealing a crispy fragile microstructure. On the other hand, the ductile failure of the fibrous specimens with central fracturing was less pronounced, as shown in Figure 15f or with the weak fiber shielding zone as shown in Figure 15i. The failure behavior of the specimens exposed to 400 °C was approximately transitional between the typical responses and those of specimens heated to 600 °C, where very tiny thermal cracks were observed on the surface of some specimens, and the central SF shielding zone of the fibrous specimens could still be recognized on the surface of the fibrous specimens as shown in Figure 15b,e,h.
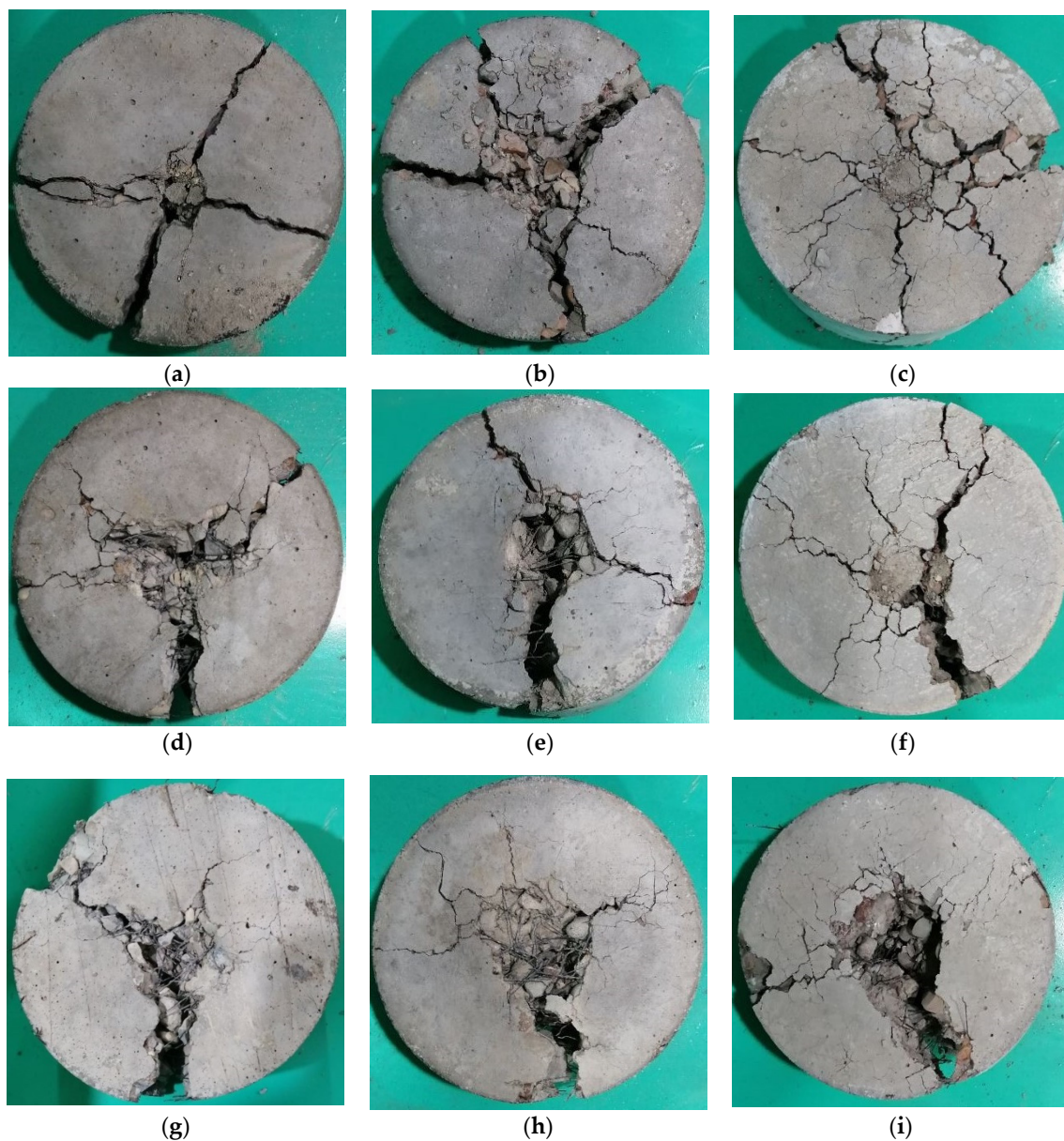

Figure 15. Failure patterns of heated specimens. (**a**) Vf = 0% 200 °C; (**b**) Vf = 0% 400 °C; (**c**) Vf = 0% 600 °C; (**d**) Vf = 0.5% 200 °C; (**e**) Vf = 0.5% 400 °C; (**f**) Vf = 0.5% 600 °C; (**g**) Vf = 1.0% 200 °C; (**h**) Vf = 1.0% 400 °C; (**i**) Vf = 1.0% 600 °C.

8. Conclusions

The following conclusions can be summarized from the experimental results obtained in this study:

1. The effect of steel-fiber (SF) inclusion was positive on compressive strength before and after exposure to high temperatures. The inclusion of 0.5% and 1.0% of hooked-end SF increased the strength (compared to plain cubes) of unheated specimens by approximately 3% and 17%, respectively, which was attributed to the stiffness enhancement gained by SF. However, this enhancement was more pronounced after exposure to high temperatures where the percentage increase was more than 30% at 600 °C for both SF contents. The additional strength percentage improvement could be attributed to the action of SF as a bridging element that connected the deteriorated microstructure of the heated specimens by crossing the thermal cracks.

2. Exposure to 200 °C increased the compressive strength of plain and fibrous specimens by more than 10%, which could be attributed to the increase in surface physical forces due to moisture loss. On the other hand, the decomposition of calcium hydroxide, and the deterioration of the bond between aggregate and cement paste led to a strength loss of approximately 27% to 43% after exposure to 600 °C.

3. SF played a major role in boosting the energy absorption capacity and resistance to repeated impacts of the concrete. A percentage development of approximately 40% to 140% of impact resistance at cracking (N_{cr}) was recorded for unheated specimens and those subjected to 200 °C when 0.5% and 1.0% SF were used. The effect of SF on N_{cr} was higher at 600 °C than that at a lower temperature, where the percentage developments were 117% and 250% due to using 0.5% and 1.0% SF, respectively, compared to plain specimens exposed to the same temperature. The better action of SF at 600 °C could be attributed to the degree of deterioration in the microstructure reached due to high thermal stresses, which enabled SF to be fully functional in bridging cracks and fragmented elements.

4. Steel fibers could provide a much higher enhancement in impact resistance at the failure stage than that at the cracking stage, which was attributed to their main function as tiny crack bridging and reinforcement elements, where their ability to help in sustaining higher tensile stresses is activated after cracking. Compared to plain specimens subjected to the same temperatures, fibrous specimens with 1.0% SF could retain higher N_f by approximately 420% for the unheated specimens, and approximately 650% to 1680% for specimens heated to the adopted high temperatures. The highest percentage development in N_f was also recorded at 600 °C.

5. The specimens heated to high temperatures were dramatically deteriorated when subjected to repeated impact loads regardless of the adopted fiber content, where even after exposure to the sub high temperature of 200 °C, the specimens lost more than 80% of their cracking impact resistance and more than 60% of their failure impact resistance, while the impact resistance was almost lost after exposure to 400 and 600 °C. The maximal residual N_{cr} and N_f percentages were 4% and 7% at 400 °C, and 2.2% and 4% at 600 °C.

6. The specimens heated to 200 °C exhibited a similar fracturing behavior to that of the unheated ones, where minimal central fracturing with line or diagonal cracks was the cause of the brittle failure of the plain specimens, while the SFs composed a central shielding zone that noticeably widened the central fracturing zone of the fibrous specimens, exhibiting more ductile behavior with SF bridged cracks. On the other hand, exposure to 600 °C altered the failure patterns that were more affected by the thermal cracking due to high-temperature exposure.

References

1. Brushlinsky, N.N.; Ahrens, M.; Sokolov, S.V.; Wagner, P. *World Fire Statistics, Center of Fire Statistics of CTIF*; International Association of Fire and Rescue Services: Ljubljana, Slovenia, 2018.
2. Arna'ot, F.H.; Abid, S.R.; Özakça, M.; Tayşi, N. Review of concrete flat plate-column assemblies under fire conditions. *Fire Saf. J.* **2017**, *93*, 39–52. [CrossRef]
3. Schneider, U. *Properties of Materials at High Temperatures—Concrete*; RILEM-Committee 44-PHT, Department of Civil Engineering, University of Kassel: Kassel, Germany, 1985.
4. Phan, L.T.; Carino, N.J. Effects of test conditions and mixture proportions on behavior of high strength concrete exposed to high temperatures. *ACI Mater. J.* **2002**, *99*, 54–66.
5. Netinger, I.; Kesegic, I.; Guljas, I. The effect of high temperatures on the mechanical properties of concrete made with different types of aggregates. *Fire Saf. J.* **2011**, *46*, 425–430. [CrossRef]
6. Albrektsson, J.; Flansbjer, M.; Lindqvist, J.E.; Jansson, R. *Assessment of Concrete Structures after Fire*; SP Report 19; SP Technical Research Institute of Sweden: Borås, Sweden, 2011.
7. Guo, Y.; Zhang, J.; Chen, G.; Xie, Z. Compressive behaviour of concrete structures incorporating recycled concrete aggregates, rubber crumb and reinforced with steel fibre, subjected to elevated temperatures. *J. Clean. Prod.* **2014**, *72*, 193–203. [CrossRef]
8. Tufail, M.; Shahzada, K.; Gencturk, B.; Wei, J. Effect of elevated temperature on mechanical properties of limestone, quartzite and granite concrete. *Int. J. Concr. Struct. Mater.* **2017**, *11*, 17–28. [CrossRef]
9. Roufael, G.; Beaucour, A.-L.; Eslami, J.; Hoxha, D.; Noumowe, A. Influence of lightweight aggregates on the physical and mechanical residual properties of concrete subjected to high temperatures. *Constr. Build. Mater.* **2021**, *268*, 121221. [CrossRef]
10. Drzymala, T.; Jackiewicz-Rek, W.; Tomaszewski, M.; Kus, A.; Galaj, J.; Sukys, R. Effects of high temperatures on the properties of high performance concrete (HPC). *Procedia Eng.* **2017**, *172*, 256–263. [CrossRef]
11. Phan, L.T.; Carino, N.J. Review of mechanical properties of HSC at elevated temperatures. *J. Mater. Civ. Eng.* **1998**, *10*, 58–64. [CrossRef]
12. Phan, L.T.; Carino, N.J. Code provisions for high strength concrete strength-temperature relationship at elevated temperatures. *Mater. Struct.* **2003**, *36*, 91–98. [CrossRef]
13. Abrams, M.S. *Compressive Strength of Concrete at Temperatures to 1600 °F*; American Concrete Institute (ACI) SP 25; Temperature and Concrete: Detroit, MI, USA, 1971.
14. Al-Owaisy, S.R. Post heat exposure properties of steel fiber reinforced concrete. *J. Eng. Sustain. Dev.* **2006**, *10*, 194–207.
15. Dügenci, O.; Haktanir, T. Experimental research for the effect of high temperature on the mechanical properties of steel fiber-reinforced concrete. *Constr. Build Mater.* **2015**, *75*, 82–88. [CrossRef]
16. Chu, H.-Y.; Jiang, J.-Y.; Sun, W.; Zhang, M. Mechanical and physicochemical properties of ferro-siliceous concrete subjected to elevated temperatures. *Constr. Build. Mater.* **2016**, *122*, 743–752. [CrossRef]
17. Deng, Z.H.; Huang, H.Q.; Ye, B.; Wang, H.; Xiang, P. Investigation on recycled aggregate concretes exposed to high temperature by biaxial compressive tests. *Constr. Build. Mater.* **2020**, *244*, 118048. [CrossRef]
18. Cheng, F.P.; Kodur, V.K.R.; Wang, T.C. Stress-strain curves for high strength concrete at elevated temperatures. *J. Mater. Civ. Eng.* **2004**, *16*, 84–94. [CrossRef]
19. Husem, M. The effects of high temperature on compressive and flexural strengths of ordinary and high-performance concrete. *Fire Saf. J.* **2006**, *41*, 155–163. [CrossRef]
20. Al-Owaisy, S.R. Strength and elasticity of steel fiber reinforced concrete at high temperatures. *J. Eng. Sustain. Dev.* **2007**, *11*, 125–133.

21. Toric, N.; Boko, I.; Peroš, B. Reduction of postfire properties of high-strength concrete. *Adv. Civ. Eng.* **2013**, *2013*, 712953.

22. Arna'ot, F.H.; Abbass, A.A.; Abualtemen, A.A.; Abid, S.R.; Özakça, M. Residual strength of high strength concentric column-SFRC flat plate exposed to high temperatures. *Constr. Build. Mater.* **2017**, *154*, 204–218. [CrossRef]

23. Sultan, H.K.; Alyaseri, I. Effects of elevated temperatures on mechanical properties of reactive powder concrete elements. *Constr. Build. Mater.* **2020**, *261*, 120555. [CrossRef]

24. Alimrani, N.; Balazs, G.L. Investigations of direct shear of one-year old SFRC after exposed to elevated temperatures. *Constr. Build. Mater.* **2020**, *254*, 119308. [CrossRef]

25. Zhang, W.; Chen, S.; Zhang, N.; Zhou, Y. Low-velocity flexural impact response of steel fiber reinforced concrete subjected to freeze-thaw cycles in NaCl solution. *Constr. Build. Mater.* **2015**, *101*, 522–526. [CrossRef]

26. Salaimanimagudam, M.P.; Suribabu, C.R.; Murali, G.; Abid, S.R. Impact response of hammerhead pier fibrous concrete beams designed with topology optimization. *Period. Polytech. Civ. Eng.* **2020**, *64*, 1244–1258. [CrossRef]

27. Zhang, W.; Chen, S.; Liu, Y. Effect of weight and drop height of hammer on the flexural impact performance of fiber-reinforced concrete. *Constr. Build. Mater.* **2017**, *140*, 31–35. [CrossRef]

28. Pan, Y.; Wu, C.; Cheng, X.; Li, V.C.; He, L. Impact fatigue behaviour of GFRP mesh reinforced engineered cementitious composites for runway pavement. *Constr. Build. Mater.* **2020**, *230*, 116898. [CrossRef]

29. Wang, W.; Chouw, N. The behaviour of coconut fibre reinforced concrete (CFRC) under impact loading. *Constr. Build. Mater.* **2017**, *134*, 452–461. [CrossRef]

30. Abid, S.R.; Gunasekaran, M.; Ali, S.H.; Kadhum, A.L.; Al-Gasham, T.S.; Fediuk, R.; Vatin, N.; Karelina, M. Impact performance of steel fiber-reinforced self-compacting concrete against repeated drop weight impact. *Crystals* **2021**, *11*, 91. [CrossRef]

31. Murali, G.; Abid, S.R.; Vatin, N.I. Experimental and Analytical Modeling of Flexural Impact Strength of Preplaced Aggregate Fibrous Concrete Beams. *Materials* **2022**, *15*, 3857. [CrossRef]

32. Hrynyk, T.D.; Vecchio, F.J. Beahvior of steel fiber-reinforced concrete slabs under impact loads. *ACI Struct. J.* **2014**, *111*, 1213–1224. [CrossRef]

33. Koutas, L.N.; Bournas, D.A. Flexural strengthening of two-way RC slabs with textile-reinforced mortar: Experimental investigation and design equations. *J. Compos. Constr.* **2017**, *21*, 04016065. [CrossRef]

34. Batran, T.Z.; Ismail, M.K.; Hassan, A.A.A. Behavior of novel hybrid lightweight concrete composites under drop-weight impact loading. *Structures* **2021**, *34*, 2789–2800. [CrossRef]

35. Batarlar, B.; Hering, M.; Bracklow, F.; Kühn, T.; Beckmann, B.; Curbach, M. Experimental investigation on reinforced concrete slabs strengthened with carbon textiles under repeated impact loads. *Structural Concrete.* **2021**, *22*, 120–131. [CrossRef]

36. Huang, Z.; Chen, W.; Tran, T.T.; Pham, T.M.; Hao, H.; Chen, Z.; Elchalakani, M. Experimental and numerical study on concrete beams reinforced with Basalt FRP bars under static and impact loads. *Compos. Struct.* **2021**, *263*, 113648. [CrossRef]

37. Said, A.M.I.; Mabrook Mouwainea, E. Experimental investigation on reinforced concrete slabs under high-mass low velocity repeated impact loads. *Structures* **2022**, *35*, 314–324. [CrossRef]

38. Gopalaratnam, V.S.; Shah, S.P.; John, R. A modified instrumented charpy test for cement-based composites. *Exp. Mech.* **1984**, *24*, 102–111. [CrossRef]

39. Yu, R.; Van Beers, L.; Spiesz, P.; Brouwers, H.J.H. Impact resistance of a sustainable Ultra-High Performance Fibre Reinforced Concrete (UHPFRC) under pendulum impact loadings. *Constr. Build. Mater.* **2016**, *107*, 203–215. [CrossRef]

40. Ziada, M.; Erdem, S.; Tammam, Y.; Kara, S.; Lezcano, R.A.G. The effect of basalt fiber on mechanical, microstructural, and high-temperature properties of fly ash-based and basalt powder waste-filled sustainable geopolymer mortar. *Sustainability* **2021**, *13*, 12610. [CrossRef]

41. *ACI 544.2R-89*; Measurement of Properties of Fiber Reinforced Concrete. American Concrete Institute: Farmington Hills, MI, USA, 1999; Volume 89, pp. 1–12.

42. Soroushian, P.; Nagi, M.; Alhozaimy, A. Statistical variations in the mechanical properties of carbon fiber reinforced cement composites. *ACI Mater. J.* **1992**, *89*, 131–138. [CrossRef]

43. Badr, A.; Ashour, A.F. Modified ACI drop-weight impact test for concrete. *ACI Mater. J.* **2005**, *102*, 249–255. [CrossRef]

44. Myers, J.J.; Tinsley, M. Impact resistance of blast mitigation material using modified aci drop-weight impact test. *ACI Mater. J.* **2013**, *110*, 339–348. [CrossRef]

45. Fakharifar, M.; Dalvand, A.; Arezoumandi, M.; Sharbatdar, M.K.; Chen, G.; Kheyroddin, A. Mechanical properties of high performance fiber reinforced cementitious composites. *Comput. Chem. Eng.* **2014**, *71*, 510–520. [CrossRef]

46. Mastali, M.; Dalvand, A.; Sattarifard, A.R. The impact resistance and mechanical properties of reinforced self-compacting concrete with recycled glass fibre reinforced polymers. *J. Clean. Prod.* **2016**, *124*, 312–324. [CrossRef]

47. Mastali, M.; Dalvand, A. The impact resistance and mechanical properties of self-compacting concrete reinforced with recycled CFRP pieces. *Compos. Part B Eng.* **2016**, *92*, 360–376. [CrossRef]

48. Mastali, M.; Dalvand, A.; Sattarifard, A. The impact resistance and mechanical properties of the reinforced self-compacting concrete incorporating recycled CFRP fiber with different lengths and dosages. *Compos. Part B Eng.* **2017**, *112*, 74–92. [CrossRef]

49. Badr, A.; Ashour, A.F.; Platten, A.K. Statistical variations in impact resistance of polypropylene fibre-reinforced concrete. *Int. J. Impact Eng.* **2006**, *32*, 1907–1920. [CrossRef]

50. Alavi Nia, A.; Hedayatian, M.; Nili, M.; Sabet, V.A. An experimental and numerical study on how steel and polypropylene fibers affect the impact resistance in fiber-reinforced concrete. *Int. J. Impact Eng.* **2012**, *46*, 62–73. [CrossRef]

51. Mohammadhosseini, H.; Alrshoudi, F.; Tahir, M.M.; Alyousef, R.; Alghamdi, H.; Alharbi, Y.R.; Alsaif, A. Performance evaluation of novel prepacked aggregate concrete reinforced with waste polypropylene fibers at elevated temperatures. *Constr. Build. Mater.* **2020**, *259*, 120418. [CrossRef]

52. Nili, M.; Afroughsabet, V. The effects of silica fume and polypropylene fibers on the impact resistance and mechanical properties of concrete. *Constr. Build. Mater.* **2010**, *24*, 927–933. [CrossRef]

53. Ismail, M.K.; Hassan, A.A.A.; Lachemi, M. Performance of Self-Consolidating Engineered Cementitious Composite under Drop-Weight Impact Loading. *J. Mater. Civ. Eng.* **2019**, *31*, 04018400. [CrossRef]

54. Ali, M.A.E.M.; Soliman, A.M.; Nehdi, M.L. Hybrid-fiber reinforced engineered cementitious composite under tensile and impact loading. *Mater. Des.* **2017**, *117*, 139–149. [CrossRef]

55. Nataraja, M.C.; Dhang, N.; Gupta, A.P. Statistical variations in impact resistance of steel fiber-reinforced concrete subjected to drop weight test. *Cem. Concr. Res.* **1999**, *29*, 989–995. [CrossRef]

56. Murali, G.; Abid, S.R.; Mugahed Amran, Y.H.; Abdelgader, H.S.; Fediuk, R.; Susrutha, A.; Poonguzhali, K. Impact performance of novel multi-layered prepacked aggregate fibrous composites under compression and bending. *Structures* **2020**, *28*, 1502–1515. [CrossRef]

57. Mahakavi, P.; Chithra, R. Impact resistance, microstructures and digital image processing on self-compacting concrete with hooked end and crimped steel fiber. *Constr. Build. Mater.* **2019**, *220*, 651–666. [CrossRef]

58. Murali, G.; Prasad, N.; Klyuev, S.; Fediuk, R.; Abid, S.R.; Amran, M.; Vatin, N. Impact resistance of functionally layered two-stage fibrous concrete. *Fibers* **2021**, *9*, 88. [CrossRef]

59. Song, P.S.; Wu, J.C.; Hwang, S.; Sheu, B.C. Statistical analysis of impact strength and strength reliability of steel-polypropylene hybrid fiber-reinforced concrete. *Constr. Build. Mater.* **2005**, *19*, 1–9. [CrossRef]

60. Song, P.S.; Wu, J.C.; Hwang, S.; Sheu, B.C. Assessment of statistical variations in impact resistance of high-strength concrete and high-strength steel fiber-reinforced concrete. *Cem. Concr. Res.* **2005**, *35*, 393–399. [CrossRef]

61. Nili, M.; Afroughsabet, V. Combined effect of silica fume and steel fibers on the impact resistance and mechanical properties of concrete. *Int. J. Impact Eng.* **2010**, *37*, 879–886. [CrossRef]

62. Rahmani, T.; Kiani, B.; Shekarchi, M.; Safari, A. Statistical and experimental analysis on the behavior of fiber reinforced concretes subjected to drop weight test. *Constr. Build. Mater.* **2012**, *37*, 360–369. [CrossRef]

63. Yildirim, S.T.; Ekinci, C.E.; Findik, F. Properties of hybrid fiber reinforced concrete under repeated impact loads 1. *Russ. J. Nondestruct. Test.* **2010**, *46*, 538–546. [CrossRef]

64. Ismail, M.K.; Hassan, A.A.A. Impact resistance and mechanical properties of self-consolidating rubberized concrete reinforced with steel fibers. *J. Mater. Civ. Eng.* **2017**, *29*, 04016193. [CrossRef]

65. AbdelAleem, B.H.; Ismail, M.K.; Hassan, A.A.A. The combined effect of crumb rubber and synthetic fibers on impact resistance of self-consolidating concrete. *Constr. Build. Mater.* **2018**, *162*, 816–829. [CrossRef]

66. Ding, Y.; Li, D.; Zhang, Y.; Azevedo, C. Experimental investigation on the composite effect of steel rebars and macro fibers on the impact behavior of high performance self-compacting concrete. *Constr. Build. Mater.* **2017**, *136*, 495–505. [CrossRef]

67. Chen, X.Y.; Ding, Y.N.; Azevedo, C. Combined effect of steel fibres and steel rebars on impact resistance of high performance concrete. *J. Cent. South Univ. Technol.* **2011**, *18*, 1677–1684. [CrossRef]

68. Murali, G.; Abid, S.R.; Abdelgader, H.S.; Amran, Y.H.M.; Shekarchi, M.; Wilde, K. Repeated Projectile Impact Tests on Multi-Layered Fibrous Cementitious Composites. *Int. J. Civ. Eng.* **2021**, *19*, 635–651. [CrossRef]

69. Haridharan, M.K.; Matheswaran, S.; Murali, G.; Abid, S.R.; Fediuk, R.; Mugahed Amran, Y.H.; Abdelgader, H.S. Impact response of two-layered grouted aggregate fibrous concrete composite under falling mass impact. *Constr. Build. Mater.* **2020**, *263*, 120628. [CrossRef]

70. Kathirvel, P.; Murali, G.; Vatin, N.I.; Abid, S.R. Experimental Study on Self Compacting Fibrous Concrete Comprising Magnesium Sulphate Solution Treated Recycled Aggregates. *Materials* **2022**, *15*, 340. [CrossRef]

71. Murali, G.; Prasad, N.; Abid, S.R.; Vatin, N.I. Response of Functionally Graded Preplaced Aggregate Fibrous Concrete with Superior Impact Strength. *Buildings* **2022**, *12*, 563. [CrossRef]

72. Vatin, N.I.; Murali, G.; Abid, S.R.; de Azevedo, A.R.G.; Tayeh, B.; Dixit, S. Enhancing the Impact Strength of Prepacked Aggregate Fibrous Concrete Using Asphalt-Coated Aggregates. *Materials* **2022**, *15*, 2598. [CrossRef]

73. Murali, G.; Abid, S.R.; Amran, M.; Vatin, N.I.; Fediuk, R. DropWeight Impact Test on Prepacked Aggregate Fibrous Concrete—An Experimental Study. *Materials* **2022**, *15*, 3096. [CrossRef]

74. Murali, G.; Abid, S.R.; Amran, M.; Fediuk, R.; Vatin, N.; Karelina, M. Combined effect of multi-walled carbon nanotubes, steel fibre and glass fibre mesh on novel two-stage expanded clay aggregate concrete against impact loading. *Crystals* **2021**, *11*, 720. [CrossRef]

75. Murali, G.; Abid, S.R.; Karthikeyan, K.; Haridharan, M.K.; Amran, M.; Siva, A. Low-velocity impact response of novel prepacked expanded clay aggregate fibrous concrete produced with carbon nano tube, glass fiber mesh and steel fiber. *Constr. Build. Mater.* **2021**, *284*, 122749. [CrossRef]

76. Ramakrishnan, K.; Depak, S.R.; Hariharan, K.R.; Abid, S.R.; Murali, G.; Cecchin, D.; Fediuk, R.; Mugahed Amran, Y.H.; Abdelgader, H.S.; Khatib, J.M. Standard and modified falling mass impact tests on preplaced aggregate fibrous concrete and slurry infiltrated fibrous concrete. *Constr. Build. Mater.* **2021**, *298*, 123857. [CrossRef]

77.   Abid, S.R.; Abdul-Hussein, M.L.; Ayoob, N.S.; Ali, S.H.; Kadhum, A.L. Repeated drop-weight impact tests on self-compacting concrete reinforced with micro-steel fiber. *Heliyon* **2020**, *6*, e03198. [CrossRef] [PubMed]

78.   Abid, S.R.; Ali, S.H.; Goaiz, H.A.; Al-Gasham, T.S.; Kadhim, A.L. Impact resistance of steel fiber-reinforced self-compacting concrete. *Mag. Civ. Eng.* **2021**, *105*, 2712–8172. [CrossRef]

79.   Abid, S.R.; Abdul Hussein, M.L.; Ali, S.H.; Kazem, A.F. Suggested modified testing techniques to the ACI 544-R repeated drop-weight impact test. *Constr. Build. Mater.* **2020**, *244*, 118321. [CrossRef]

80.   Jabir, H.A.; Abid, S.R.; Murali, G.; Ali, S.H.; Klyuev, S.; Fediuk, R.; Vatin, N.; Promakhov, V.; Vasilev, Y. Experimental tests and reliability analysis of the cracking impact resistance of uhpfrc. *Fibers* **2020**, *8*, 74. [CrossRef]

81.   Schrader, E.K. Impact Resistance and Test Procedure for Concrete. *J. Am. Concr. Inst.* **1981**, *78*, 141–146. [CrossRef]

82.   Mehdipour, S.; Nikbin, I.M.; Dezhampanah, S.; Mohebbi, R.; Moghadam, H.; Charkhtab, S.; Moradi, A. Mechanical properties, durability and environmental evaluation of rubberized concrete incorporating steel fiber and metakaolin at elevated temperatures. *J. Clean Prod.* **2020**, *254*, 120126. [CrossRef]

83.   Al-ameri, R.A.; Abid, S.R.; Murali, G.; Ali, S.H.; Özakça, M. Residual repeated impact strength of concrete exposed to elevated temperatures. *Crystals* **2021**, *11*, 941. [CrossRef]

84.   Al-Ameri, R.A.; Abid, S.R.; Murali, G.; Ali, S.H.; Özakça, M.; Vatin, N.I. Residual Impact Performance of ECC Subjected to Sub-High Temperatures. *Materials* **2022**, *15*, 454. [CrossRef]

85.   Al-Ameri, R.A.; Abid, S.R.; Özakça, M. Mechanical and Impact Properties of Engineered Cementitious Composites Reinforced with PP Fibers at Elevated Temperatures. *Fire* **2022**, *5*, 3. [CrossRef]

86.   Foglar, M.; Hajek, R.; Fladr, J.; Pachman, J.; Stoller, J. Full-scale experimental testing of the blast resistance of HPFRC and UHPFRC bridge decks. *Constr. Build. Mater.* **2017**, *145*, 588–601. [CrossRef]

87.   Yoo, D.Y.; Banthia, N. Mechanical and structural behaviors of ultra-high-performance fiber-reinforced concrete subjected to impact and blast. *Constr. Build. Mater.* **2017**, *149*, 416–431. [CrossRef]

88.   Sun, D.; Xu, Y.; Wang, P.; Zhou, J.; Jin, F.; Li, H.; Fan, H. Blast responses of carbon-fiber reinforced polymer tubular columns filled with seawater sea-sand concrete. *Compos. Struct.* **2021**, *278*, 114692. [CrossRef]

89.   Abada, M.; Ibrahim, A.; Jung, S.J. Improving Blast Performance of Reinforced Concrete Panels Using Sacrificial Cladding with Hybrid-Multi Cell Tubes. *Modelling* **2021**, *2*, 149–165. [CrossRef]

90.   Prasad, N.; Murali, G.; Abid, S.R.; Vatin, N.; Fediuk, R.; Amran, M. Effect of Needle Type, Number of Layers on FPAFC Composite against Low-Velocity Projectile Impact. *Buildings* **2021**, *11*, 668. [CrossRef]

91.   Liu, J.; Li, J.; Fang, J.; Su, Y.; Wu, C. Ultra-high performance concrete targets against high velocity projectile impact—A-state-of-the-art review. *Int. J. Impact Eng.* **2022**, *160*, 104080. [CrossRef]

92.   Lee, M.; Park, G.K.; Kim, S.W.; Kwak, H.G. Damage characteristics of high performance fiber-reinforced cement composites panels subjected to projectile impact. *Int. J. Mech. Sci.* **2022**, *214*, 106919. [CrossRef]

93.   Feng, J.; Gao, X.; Li, J.; Dong, H.; He, Q.; Liang, J.; Sun, W. Penetration resistance of hybrid-fiber-reinforced high-strength concrete under projectile multi-impact. *Constr. Build. Mater.* **2019**, *202*, 341–352. [CrossRef]

94.   Mina, A.L.; Petrou, M.F.; Trezos, K.G. Resistance of an optimized ultra-high performance fiber reinforced concrete to projectile impact. *Buildings* **2021**, *11*, 63. [CrossRef]

95.   Lankard, D.R.; Birkimer, D.L.; Fondriest, F.F.; Snyder, M.J. *Effect of Moisture Content on the Structural Properties of Portland Cement Concrete Exposed to Temperatures Up to 500F*; ACI Special Publication SP-25; Temperature and Concrete: Detroit, MI, USA, 1971; pp. 59–102.

96.   Abid, S.R.; Abbass, A.A.; Murali, G.; Al-Sarray, M.L.J.; Nader, I.A.; Ali, S.H. Repeated Impact Response of Normal- and High-Strength Concrete Subjected to Temperatures up to 600 °C. *Materials* **2022**, *15*, 5283. [CrossRef]

97.   Zoldners, N.G. *Thermal Properties of Concrete under Sustained Elevated Temperatures*; ACI Special Publication SP-25; Temperature and Concrete: Detroit, MI, USA, 1971; pp. 1–31.